

BEMPS –

Bozen Economics & Management  
Paper Series

NO 104/ 2024

A three-way dynamic panel  
regression model for change  
point detection in  
bioimpedance data

F. Marta L. Di Lascio, Selene Perazzini

# A three-way dynamic panel threshold regression model for change point detection in bioimpedance data

F. Marta L. Di Lascio\*, Selene Perazzini †

## Abstract

Bioimpedance refers to the measurement of the electrical impedance of biological tissue and it can be used to monitor its physio-chemical changes with important implications in a wide range of applications, including bioengineering and medical diagnostics. Recently bioimpedance analysis is gaining popularity in the food industry due to its ability to provide accurate and timely information about food quality, thereby reducing waste and improving product quality.

Motivated by an original experiment on fruit bioimpedance, we develop a three-way panel dynamic threshold model and propose it as a method to detect the change point, i.e. fruit ripening time. We develop an estimation method based on the generalized method of moments and the instrumental variables estimator, and define a criterion to compute the change point. The performance of the proposed model is investigated through an extensive Monte Carlo simulation study in terms of the accuracy of both coefficients' and thresholds' estimates and the change point detected. The developed method is applied to an innovative fruit bioimpedance panel data set from two different electrical impedance analyzers, a bench-top device and a portable device. The method provides significant threshold and meaningful ripeness times. The new model is implemented and available through the R package `PanelTM`.

**Keywords:** Bioimpedance, Change point detection, FD-IV-GMM, Three-way dynamic panel model, Threshold model

**JEL Code:** C13, C18, C23, L66

## 1 Introduction

Food quality control is extremely important to ensure food safety, reduce waste, and improve product quality. Sensory evaluation of food quality is nowadays essential in the food industry to constantly monitor physio-chemical changes of the biological tissue that can be crucial to ensure the quality of the final product (see, e.g., Tománek et al., 2010; Ibba, 2021; Casa et al., 2022).

In recent years, bioimpedance is gaining popularity in the context of food quality and fruit ripening due to its ability to provide accurate and timely information about food quality (Pliquett, 2010). Indeed, bioimpedance refers to the measurement of the electrical impedance of biological tissue, that is a physical quantity describing the ability of the tissue to oppose an external flow of electrical current (Grimnes and Martinsen, 2015). The measurement technique involves applying a small electrical current to biological tissue or material and measuring the resulting electrical response. Since the electrical properties of the fruit or other food products can be correlated with specific quality attributes (see, e.g., El Khaled et al., 2017), e.g. fruit ripening, the analysis of the electrical signals are useful to provide information about the properties of the analysed tissue. Bioimpedance measurements can be performed over a range of frequencies, known as electrical impedance spectroscopy (EIS) (Grossi and Riccò, 2017). In the context of fruit quality assessment, EIS is an emerging technique for fruit quality assessment at different frequencies, as it can be used to monitor changes in the electrical properties of fruit tissues and, in turn, in their physio-chemical properties, in a non-destructive and non-invasive way due to the fact that different electrical frequencies cross cell membranes differently (Ibba et al., 2020). Thus EIS has the potential to play an important role in the food industry in the future since it can be used for quality control of fruit during storage, transportation, and processing.

---

\*Faculty of Economics and Management, Free University of Bozen-Bolzano, Piazza Università, 1 - 39100, Bozen-Bolzano, Italy, e-mail: [marta.dilascio@unibz.it](mailto:marta.dilascio@unibz.it).

†AXES Research Unit, IMT School for Advanced Studies Lucca, Italy, email: [selene.perazzini@imtlucca.it](mailto:selene.perazzini@imtlucca.it)

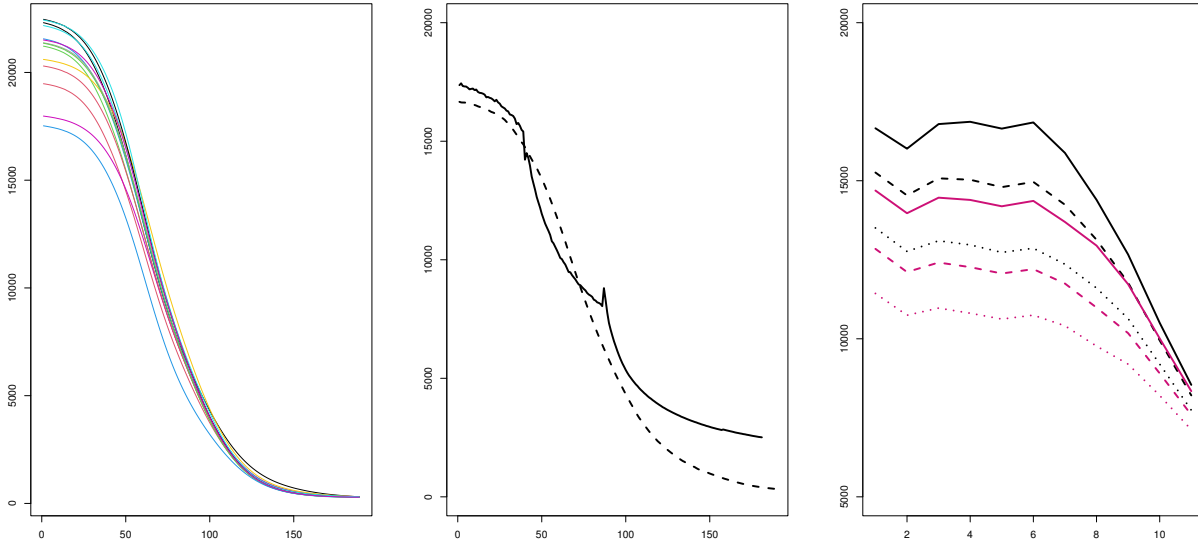


Figure 1: Bioimpedance spectra for a subset of the analysed bananas sample, a fixed instant time ( $t = 7$ ), and the IA (left); bioimpedance spectra (averaged over time and bananas) for the considered EIS device, i.e. IA (dashed line) and FM (solid line) (middle); bioimpedance time series (averaged on bananas) for a small subset of the possible frequencies for the considered EIS, i.e. IA (black lines) and FM (pink lines) (right).

In this paper we focus on multi-frequency EIS devices that measure the impedance of the system over time, that is, apply a range of frequencies to the tissue and measure the voltage response over time. In this way, time-domain EIS makes it possible to provide also insights into dynamic changes in the electrical properties of fruit. In particular, we consider two EIS devices, a bench-top impedance analyzer (IA) and a portable EIS system, called “FruitMeter” (FM) (see Sect. 2 for details). The two devices are used to study fruit samples with the aim of characterizing the physiological state of fruit, e.g. the ripeness state. From a statistical point of view, time-domain multi-frequency EIS data introduce some challenges that have to be carefully addressed. The most important are concerned with the data complexity structure since bioimpedance data present both serial and cross-sectional dependence, and are observed hundreds of times according to the range of frequencies applied. Fig. 1 graphically illustrates some bioimpedance spectra recorded for a sample of bananas, for the two different impedance analyzers, and over time. It is evident that the variability among fruits, the type of bioimpedance analyzer, and the temporal dynamics of the measurements done have an effect on bioimpedance. Hence the development of a three-way dynamic panel regression model able to keep into account the two types of dependence and the three-way data structure appears to be necessary. It is advantageous to have a dynamic model that is not only more flexible, but it also allows us to exploit the historical dynamics information by introducing lagged dependent variables among the regressors. Since one of the main purposes of fruit bioimpedance analysis is to assess the ripening time, another challenge concerns the development of a method to detect a possible point of change in the bioimpedance time series by exploiting thresholds varying across time series. The change point can be interpreted as the ripening time of fruit and, thus, it results in crucial information for the usefulness of the bioimpedance data analysis. This implies that the three-way dynamic panel regression model to develop should be a threshold regression model with a criterion for change point detection. Our proposal embraces, on the one side, panel regression models and, on the other side, change point detection methods. The reference literature is very extensive but, to the best of our knowledge, there is still a gap for change point detection in three-way panel data with temporal dynamics and thresholds varying across time series. From self-exciting threshold autoregressive models (Tong, 1990; Hansen, 2000) to the more recent dynamic panel model with threshold effect and endogeneity developed by Seo and Shin (2016), from which we were inspired, there are no panel models that work with three-way data and define threshold parameters that are not in common to all time series, although there are a variety of multi-dimensional panel models (see, e.g., Mátyás,

1997, Mátyás, 2017, Balazsi et al., 2018, and references therein). As for change point detection methods for panel data, the attempts to extend the seminal work by Bai (2010) defining a panel model with structural breaks resulted in models computationally unfeasible, see e.g. Li et al. (2015). Many contributions with different approaches have been developed (see, e.g., Chen and Huang, 2017 and Maciak et al., 2020), but each requires the introduction of restrictions to deal with the high number of parameters involved. In order to simplify the framework of the analysis, alternative approaches have tried to collapse the panel change point detection into a better-known time series problem (see, e.g., Horvath and Hušková, 2012, Chan et al., 2013, Cho, 2016), or to analyse each series of the panel separately (see, e.g., Bardwell et al., 2016). Anyway, all these methods might fail to capture change points that affect only a subset of the series in the panel. To sum up, existing methods for change-point detection are not suitable for three-way structured data and have never been applied to bioimpedance data.

To overcome the mentioned limitations of the models available in the literature, we develop a three-way panel regression model with time-varying (exogenous and/or endogenous) regressors that makes it possible to have the lagged dependent variable as transition variable and to vary the threshold parameter by the value of the third way. We also provide a measure to identify a change point in the estimated temporal dynamics. Hence we first develop a general three-way dynamic panel threshold model for change point detection that can be used in any context where the interest focuses on multi-way data and the assessment of two different regimes. Second, we analyse an innovative dataset concerning fruit bioimpedance curves over a range of frequencies. Here the purpose is twofold: we detect the ripening time and assess the possible effect of the frequency on the fruit bioimpedance; next, we compare the results obtained from two different EIS devices with the aim of providing insights on the quality of the more user-friendly and possibly low-cost portable EIS tool.

The paper is organized as follows. In Section 2 we describe the bioimpedance data which motivates our proposal. In Section 3 we present the developed three-way dynamic panel threshold model and propose a criterion to detect a change point. Moreover, we develop the generalized method of moments estimator in the instrumental variables framework including, in the appendix, the related asymptotic theory and a linear test for the threshold effect. Finite sample performance of the proposed model and its GMM estimator is examined in Section 5 where they are empirically investigated through Monte Carlo simulations. The usefulness of our proposal for real data analysis concerning bioimpedance is shown in Section 6. Discussion and conclusion are presented in Section 7.

## 2 Bioimpedance data

The innovative data we consider in this study consists of a collection of bioimpedance measurements of a production batch of 150 bananas observed for 11 days. The experiment has been conducted by the Sensing Technologies Laboratory at the Free University of Bozen-Bolzano in the context of an interdisciplinary research project between the Faculty of Economics and Management and the Faculty of Engineering. Bioimpedance is typically measured by using a bioimpedance analyzer, an instrument specifically designed for this purpose. In the experiment on fruit ripening, two bioimpedance analyzers have been used: a bench-top EIS device called “impedance analyzer” (IA) that is a marketed equipment, and an innovative portable custom-made device called “FruitMeter” (FM) (Ibba et al., 2021). Bench-top EIS devices are typically unwieldy and more powerful than a portable EIS device and, therefore, are generally more expensive and require more maintenance and expertise to operate. On the contrary, portable EIS devices are small, lightweight instruments that can be easily transported and easily used in a wide range of situations and applications. With both the analyzers, bioimpedance measurements have been performed over a range of frequencies using two electrodes placed on the surface of each fruit being measured (Ibba et al., 2020). A small alternating current is applied through one electrode and the resulting voltage is measured at the other electrode and then used to calculate the impedance of the material at different frequencies. Since the voltage that generates the flow affects the measurement of bioimpedance, multiple electrical frequencies should be considered when assessing fruit quality (Ibba et al., 2020; Ibba, 2021).

Bioimpedance measurements have been provided at 189 frequencies ranging from 20 to 13668764.956 Hz for the IA and at 181 frequencies from 10 to 99000 Hz for the FM. It is to be noted that frequency values for the IA and FM are similar but do not perfectly coincide. All the fruits were harvested simul-

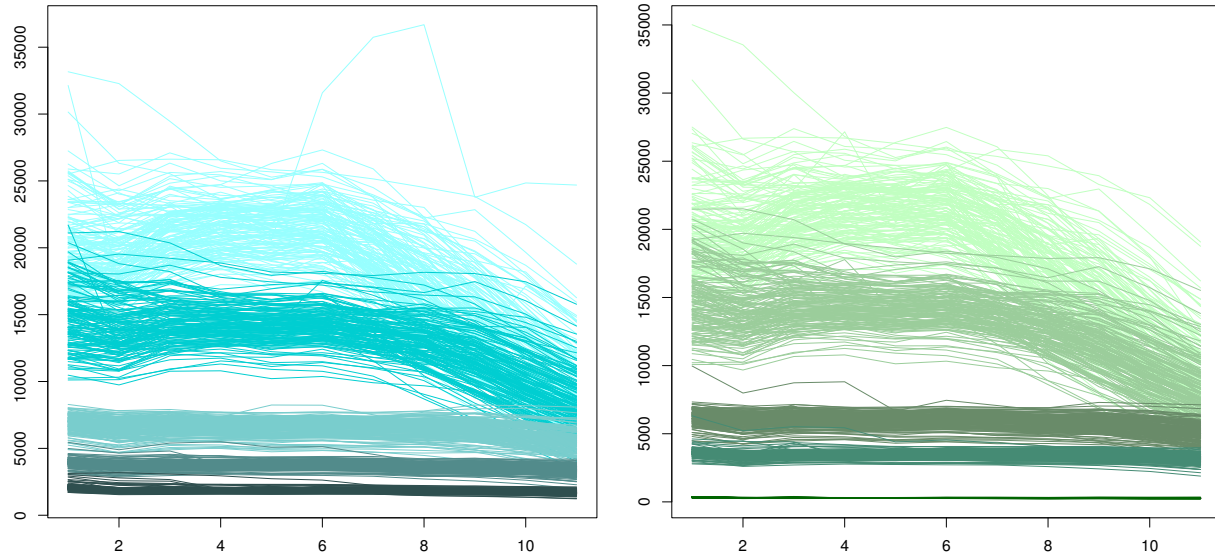


Figure 2: Bioimpedance time series of the 150 observed bananas as provided by the FM (left) and the IA (right) device by varying spectroscopy frequency among (10, 1000, 10000, 30000, 99000) Hz for FM and (20, 1018.568, 10026.058, 29286.314, 13668764.956) Hz for IA (from the lightest to the darkest colour).

taneously and marketed together, thus ensuring the homogeneity of the initial stage of ripening of the banana batch. The measurements have been performed every day for 11 days, i.e. until the fruit has visibly deteriorated, to monitor the progress of ripening under controlled room temperature and humidity. In Fig. 2 a preliminary representation of the data is shown for a set of frequencies ranging from the minimum to the maximum of the devices and considering three intermediate frequencies in common to the two used analyzers. Specifically, we considered (10, 1000, 10000, 30000, 99000) frequencies for FM and (20, 1018.568, 10026.058, 29286.314, 13668764.956) frequencies for IA.

Considering that we aim at, not only, investigating the temporal dynamics of fruit bioimpedance by varying spectroscopy frequency, but also comparing the two considered analyzers, frequencies  $j < 20$  and  $j > 99000$  Hz have been neglected. In addition, as shown in Fig. 2, we observe that bioimpedance time series tend to flatten at higher frequencies, irrespective of the type of impedance analyzer used. Even though for very high frequencies there is still variability over time, the behaviour of the bioimpedance measurements appears to be less informative in terms of the fruit ripening process. For this reason, we restrict the analysis to the set of frequencies in the interval  $20 \leq j \leq 30000$  Hz. This selection led to 103 frequencies for the IA and 107 for the FM. In the end, the two post-processing data sets constitute three-way balanced panels with  $n = 150$  bananas,  $J = 103$  and  $J = 107$  electrical frequencies for the IA and the FM, respectively, and  $T = 11$  days. Finally, we have additional information regarding fruit weight for each day, which is a time-varying regressor that can be useful in describing the fruit ripening process.

### 3 Three-way dynamic panel threshold model

We define a three-way dynamic panel threshold regression model on  $i = 1, \dots, n$  statistical units observed in  $t = 1, \dots, T$  instants of time by varying a third-way of  $j = 1, \dots, J$  values:

$$y_{ijt} = (1, \mathbf{x}'_{ijt})\phi_{1j}\mathbb{1}\{y_{ij(t-1)} \leq \gamma_j\} + (1, \mathbf{x}'_{ijt})\phi_{2j}\mathbb{1}\{y_{ij(t-1)} > \gamma_j\} + \varepsilon_{ijt} \quad (1)$$

where  $y_{ijt}$  is the value of the variable  $Y$  observed on the  $i$ -th statistical unit at time  $t$  for the  $j$ -th value of the considered third-way,  $\mathbf{x}_{ijt}$  is a vector of  $k_1$  time-varying (exogenous or endogenous) regressors, which may include lagged dependent variable,  $\phi_{1j} = (\phi_{1j}^{(1)}, \dots, \phi_{1j}^{(k_1+1)})$  and  $\phi_{2j} = (\phi_{2j}^{(1)}, \dots, \phi_{2j}^{(k_1+1)})$  are, respectively, the lower and upper regime intercept and slope parameters vectors of the  $j$ -th value,  $\mathbb{1}$  is the indicator

function that captures the change in regime and is defined by the threshold parameter  $\gamma_j$  that can vary by  $j$ , the lagged dependent variable  $y_{ij(t-1)}$  is the endogenous transition variable, and  $\varepsilon_{ijt}$  is the error term that is defined as the sum of three components:

$$\varepsilon_{ijt} = \mu_i + \lambda_j + \nu_{ijt}$$

where  $\mu_i$  is the unobserved individual fixed effect,  $\lambda_j$  is the unobserved third-way fixed effect, and  $\nu_{ijt}$  is a zero mean random error such that  $E(\nu_{ijt}|\mathcal{F}_{t-1}) = 0$ , where  $\mathcal{F}_t$  is a natural filtration at time  $t$  such that  $\nu_{ijt}$  is a martingale difference sequence.

### 3.1 GMM estimation method for the three-way model

The proposed model in Eq. (1) can be estimated by extending to the three-way model case the generalized method of moments (GMM) in [Seo and Shin \(2016\)](#), that is based on the first difference transformation (FD) and the use of instrumental variables (IVs). Inspired by the motivating empirical applications (see Sect. 6), we assume that the  $J$  values of the third way are independent of each others and represent, for instance, the categories or levels of a variable. This case occurs every time replicated observations on the same statistical units  $i$  at a fixed time  $t$  do not have any effect on each other, i.e. are independent.

The FD-IV-GMM estimator for the three-way panel threshold model in Eq. (1) is developed through a procedure for the following first-differentiated model to deal with the correlation between regressors and the individual and category fixed effects:

$$\Delta y_{ijt} = y_{ijt} - y_{ij(t-1)} = \beta_j' \Delta x_{ijt} + \delta_j' \mathbf{X}'_{ijt} \mathbb{1}_{ijt}(\gamma_j) + \Delta \varepsilon_{ijt}$$

where  $\Delta$  is the first difference operator,  $\beta_j = (\phi_{1j}^{(2)}, \dots, \phi_{1j}^{(k_1+1)})'$ ,  $\delta_j = (\phi_{2j} - \phi_{1j})$ ,

$$\mathbf{X}_{ijt} = \begin{pmatrix} (1, \mathbf{x}'_{ijt}) \\ (1, \mathbf{x}'_{ij(t-1)}) \end{pmatrix}, \mathbb{1}_{ijt}(\gamma_j) = \begin{pmatrix} \mathbb{1}\{y_{ij(t)} > \gamma_j\} \\ -\mathbb{1}\{y_{ij(t-1)} > \gamma_j\}, \end{pmatrix}$$

and  $\Delta \varepsilon_{ijt} = \varepsilon_{ijt} - \varepsilon_{ij(t-1)} = \nu_{ijt} - \nu_{ij(t-1)}$ . Hence,  $\theta_j = (\beta_j', \delta_j', \gamma_j)'$  is the  $(2k_1 + 2)$ -dimensional vector of parameters to estimate for each level  $j$ , and the whole unknown parameters vector is  $\theta = (\theta_1', \dots, \theta_J)'$  and belongs to a compact set  $\Theta \subset \mathbb{R}^{kJ}$  with  $k = (2k_1 + 2)$ .

In light of the independence among levels of the third way, we can estimate the parameters vector for each level  $j$  taken separately, i.e. estimate  $\theta_j$  for each  $j \in \{1, \dots, J\}$ . Indeed, the GMM objective function to minimize to find  $\theta$  is a block diagonal matrix where each block is positive definite and can be minimized independently from the other blocks. Hence the two-step GMM estimator can be found minimizing a GMM estimator for each  $\theta_j$ , with  $j = 1, \dots, J$  as described in the following.

For a chosen  $j$ , a two-step procedure is developed. In the first step of the estimation procedure, the following GMM estimator of  $\beta_j$  and  $\delta_j$  for a fixed  $\gamma_j$  is defined through the grid search algorithm by exploiting  $l$  instruments:

$$\left( \hat{\beta}_j(\gamma_j), \hat{\delta}_j(\gamma_j) \right) = \left( \bar{\mathbf{g}}_{2n}^{(j)}(\gamma_j)' \mathbf{W}_n^{(j)} \bar{\mathbf{g}}_{2n}^{(j)}(\gamma_j) \right)^{-1} \bar{\mathbf{g}}_{2n}^{(j)}(\gamma_j)' \mathbf{W}_n^{(j)} \bar{\mathbf{g}}_{1n}^{(j)}(\gamma_j)$$

where  $\bar{\mathbf{g}}_{1n}^{(j)}(\gamma_j) = \frac{1}{n} \sum_{i=1}^n \mathbf{g}_{1i}^{(j)}$  with

$$\mathbf{g}_{1i}^{(j)} = \begin{pmatrix} z_{ijt_0} \Delta y_{ijt_0} \\ \vdots \\ z_{ijT} \Delta y_{ijT}, \end{pmatrix}$$

$\bar{\mathbf{g}}_2^{(j)}(\gamma_j) = \frac{1}{n} \sum_{i=1}^n \mathbf{g}_{2i}^{(j)}(\gamma_j)$  with

$$\mathbf{g}_{2i}^{(j)}(\gamma_j) = \begin{pmatrix} z_{ijt_0} (\Delta x_{ijt_0}, \mathbb{1}_{ijt_0}(\gamma_j)' \mathbf{X}_{ijt_0}) \\ \vdots \\ z_{ijT} (\Delta x_{ijT}, \mathbb{1}_{ijT}(\gamma_j)' \mathbf{X}_{ijT}), \end{pmatrix}$$

$\{z_{ijt}\}_{t=t_0}^T$  is the set of  $l$  instrumental variables  $\forall j$ , and  $\mathbf{W}_n^{(j)}$  is a  $(l \times l)$  weight matrix whose form can be specified in different ways. Following [Seo and Shin \(2016\)](#), it can be either  $\mathbf{W}_n^{(j)} = \mathbf{I}_l$  or as follows:

$$\mathbf{W}_n^{(j)} = \begin{pmatrix} \frac{2}{n} \sum_{i=1}^n z_{ijt_0} z'_{ijt_0} & -\frac{1}{n} \sum_{i=1}^n z_{ijt_0} z'_{ijt_0+1} & 0 & \dots \\ -\frac{1}{n} \sum_{i=1}^n z_{ijt_0+1} z'_{ijt_0} & \frac{2}{n} \sum_{i=1}^n z_{ijt_0+1} z'_{ijt_0+1} & \ddots & \ddots \\ 0 & \ddots & \ddots & -\frac{1}{n} \sum_{i=1}^n z_{ijT-1} z'_{ijT} \\ \dots & \ddots & -\frac{1}{n} \sum_{i=1}^n z_{ijT} z'_{ijT-1} & \frac{2}{n} \sum_{i=1}^n z_{ijT} z'_{ijT} \end{pmatrix}^{-1}.$$

The GMM estimator of  $\gamma_j$  is then obtained as follows:

$$\hat{\gamma}_j = \arg \min_{\gamma_j \in \Gamma_j} \hat{\mathbf{J}}_n^{(j)}(\gamma_j)$$

where  $\hat{\mathbf{J}}_n^{(j)}(\gamma_j)$  denotes the objective function evaluated at  $\hat{\beta}_j(\gamma_j)$  and  $\hat{\delta}_j(\gamma_j)$ , given by  $\hat{\mathbf{J}}_n^{(j)}(\gamma_j) = \bar{\mathbf{g}}_n^{(j)}(\gamma_j)' \mathbf{W}_n^{(j)} \bar{\mathbf{g}}_n^{(j)}(\gamma_j)$ , and the  $(l \times 1)$  vector of sample moment conditions is defined as follows:

$$\begin{aligned} \bar{\mathbf{g}}_n^{(j)}(\gamma_j) &= \bar{\mathbf{g}}_{1n}^{(j)} - \bar{\mathbf{g}}_{2n}^{(j)}(\gamma_j) \left( \hat{\beta}_j(\gamma_j)', \hat{\delta}_j(\gamma_j)' \right)' \\ &= \frac{1}{n} \sum_{i=1}^n \mathbf{g}_{1i}^{(j)} - \frac{1}{n} \sum_{i=1}^n \mathbf{g}_{2i}^{(j)}(\gamma_j) \left( \hat{\beta}_j(\gamma_j)', \hat{\delta}_j(\gamma_j)' \right)'. \end{aligned}$$

The first-step GMM parameters estimates then are  $(\hat{\beta}_j', \hat{\delta}_j', \hat{\gamma}_j)'$  where  $(\hat{\beta}_j', \hat{\delta}_j')' = (\hat{\beta}_j(\hat{\gamma}_j)', \hat{\delta}_j(\hat{\gamma}_j)')'$ .

The second-step GMM estimators are given by the procedure based on the grid search algorithm described above updated by exploiting the first-step estimates. Hence, the (final) GMM estimator of  $\theta_j$ , which is  $\hat{\theta}_j$ , is obtained as follows:

$$\hat{\theta}_j = \arg \min_{\theta_j \in \Theta_j} \hat{\mathbf{J}}_n^{(j)}(\theta_j)$$

where

$$\hat{\mathbf{J}}_n^{(j)}(\theta_j) = \bar{\mathbf{g}}_n^{(j)}(\theta_j)' \mathbf{W}_n^{(j)} \bar{\mathbf{g}}_n^{(j)}(\theta_j) \quad (2)$$

with  $\mathbf{W}_n^{(j)} = \left( \frac{1}{n} \sum_{i=1}^n \hat{\mathbf{g}}_i^{(j)}(\theta_j) \hat{\mathbf{g}}_i^{(j)'}(\theta_j) - \frac{1}{n^2} \sum_{i=1}^n \hat{\mathbf{g}}_i^{(j)}(\theta_j) \sum_{i=1}^n \hat{\mathbf{g}}_i^{(j)'}(\theta_j) \right)^{-1}$ ,

$$\begin{aligned} \hat{\mathbf{g}}_i^{(j)}(\theta_j) &= \begin{pmatrix} z_{ijt_0} \left( \Delta y_{ijt_0} - \hat{\beta}_j' \Delta \mathbf{x}_{ijt_0} - \hat{\delta}_j' \mathbf{X}'_{ijt_0} \mathbf{1}_{ijt_0}(\hat{\gamma}_j) \right) \\ \vdots \\ z_{ijT} \left( \Delta y_{ijT} - \hat{\beta}_j' \Delta \mathbf{x}_{ijT} - \hat{\delta}_j' \mathbf{X}'_{ijT} \mathbf{1}_{ijT}(\hat{\gamma}_j) \right) \end{pmatrix} \\ &= \left( \widehat{\Delta \varepsilon}_{ijt} z'_{ijt_0}, \dots, \widehat{\Delta \varepsilon}_{ijt} z'_{ijT} \right), \end{aligned}$$

and  $\widehat{\Delta \varepsilon}_{ijt}$  are the residuals obtained from the first-step estimation. The described estimation procedure is repeated for each value of  $j$  to obtain the FD-IV-GMM estimates  $\hat{\theta}$  of all the parameters in the three-way model in Eq. (1).

As previously mentioned, we assume independence between third-way's levels and, consequently, the  $(lJ \times lJ)$  weight matrix  $\mathbf{W}$  is a diagonal block matrix whose blocks on the diagonal are given by a  $(l \times l)$  weight matrix  $\mathbf{W}_n^{(j)}$  concerning the  $j$ -th level. Hence, the whole parameters vector  $\theta$  is estimated by applying the above described GMM estimator for each  $\theta_j$  taken separately, where  $j = 1, \dots, J$ . Specifically, the closed-form solution to produce GMM estimates of the whole parameters vector  $\hat{\theta}$  is in the diagonal of the following

matrix:

$$\begin{aligned}
\hat{\mathbf{J}}(\boldsymbol{\theta}) &= \begin{pmatrix} \bar{\mathbf{g}}_n^{(1)}(\boldsymbol{\theta}_1)' & \mathbf{0} & \dots & \dots & \mathbf{0} \\ \vdots & \ddots & \vdots & \dots & \vdots \\ \mathbf{0} & \dots & \bar{\mathbf{g}}_n^{(j)}(\boldsymbol{\theta}_j)' & \dots & \mathbf{0} \\ \vdots & \dots & \dots & \ddots & \vdots \\ \mathbf{0} & \dots & \dots & \mathbf{0} & \bar{\mathbf{g}}_n^{(J)}(\boldsymbol{\theta}_J)' \end{pmatrix} \begin{pmatrix} \mathbf{W}_n^{(1)} & \mathbf{0} & \dots & \dots & \mathbf{0} \\ \vdots & \ddots & \vdots & \dots & \vdots \\ \mathbf{0} & \dots & \mathbf{W}_n^{(j)} & \dots & \mathbf{0} \\ \vdots & \dots & \dots & \ddots & \vdots \\ \mathbf{0} & \dots & \dots & \mathbf{0} & \mathbf{W}_n^{(J)} \end{pmatrix} \\
&= \begin{pmatrix} \bar{\mathbf{g}}_n^{(1)}(\boldsymbol{\theta}_1) & \mathbf{0} & \dots & \dots & \mathbf{0} \\ \vdots & \ddots & \vdots & \dots & \vdots \\ \mathbf{0} & \dots & \bar{\mathbf{g}}_n^{(j)}(\boldsymbol{\theta}_j) & \dots & \mathbf{0} \\ \vdots & \dots & \dots & \ddots & \vdots \\ \mathbf{0} & \dots & \dots & \dots & \bar{\mathbf{g}}_n^{(J)}(\boldsymbol{\theta}_J) \end{pmatrix} \\
&= \begin{pmatrix} \hat{\mathbf{J}}_n^{(1)}(\boldsymbol{\theta}_1) & \mathbf{0} & \dots & \dots & \mathbf{0} \\ \vdots & \ddots & \vdots & \dots & \vdots \\ \mathbf{0} & \dots & \hat{\mathbf{J}}_n^{(j)}(\boldsymbol{\theta}_j) & \dots & \mathbf{0} \\ \vdots & \dots & \dots & \ddots & \vdots \\ \mathbf{0} & \dots & \dots & \mathbf{0} & \hat{\mathbf{J}}_n^{(J)}(\boldsymbol{\theta}_J) \end{pmatrix} \tag{3}
\end{aligned}$$

where  $\hat{\mathbf{J}}_n^{(j)}(\boldsymbol{\theta}_j) = \bar{\mathbf{g}}_n^{(j)}(\boldsymbol{\theta}_j)' \mathbf{W}_n^{(j)} \bar{\mathbf{g}}_n^{(j)}(\boldsymbol{\theta}_j)$  with  $j = 1, \dots, J$ . Hence,

$$\hat{\boldsymbol{\theta}} = \left( \arg \min_{\boldsymbol{\theta}_1 \in \Theta_1} \hat{\mathbf{J}}_n^{(1)}(\boldsymbol{\theta}_1), \dots, \arg \min_{\boldsymbol{\theta}_j \in \Theta_j} \hat{\mathbf{J}}_n^{(j)}(\boldsymbol{\theta}_j), \dots, \arg \min_{\boldsymbol{\theta}_J \in \Theta_J} \hat{\mathbf{J}}_n^{(J)}(\boldsymbol{\theta}_J) \right) \tag{4}$$

where  $\hat{\mathbf{J}}_n^{(j)}(\boldsymbol{\theta}_j)$  is as given in Eq. (2) and subsequent equations.

The asymptotic theory of the estimator in Eq. (4) and the test for threshold effect are developed in Appendices A and B, respectively.

## 4 Change point detection

The three-way dynamic panel threshold model in Eq. (1) is also thought to detect change points in panel data. Once the proposed model is estimated through the method developed in Sect. 3, the final goal is to compute the change point (CP) in each time series, that is the time at which a regime switch occurs. From the applied point of view, this concerns testing structural change problems that occur naturally in many contexts; for example, in fruit ripening control context, where one is faced with the output of a production line and wants to detect any departure from an acceptable production standard. We propose to compute the change point as the minimum time at which the regime switch occurs, that is, at which the time series is greater than the estimated threshold parameter. We thus define the following measure:

$$\widehat{\text{CP}}_{ij} = \arg \min_{t \in \{1, \dots, T\}} \{\mathbf{1}(y_{ijt} > \hat{\gamma}_j)\} \tag{5}$$

that provides the time of the regime change  $\forall i, j$ , i.e. for each time series and frequency of the spectroscopy, and, next, we summarize  $\widehat{\text{CP}}_{ij}$  over  $i$  as follows:

$$\widehat{\text{CP}}_j = \sum_{i=1}^n \frac{\widehat{\text{CP}}_{ij}}{n}. \tag{6}$$

In this way, measures in Eqs. (5) and (6) make it possible to assess the time of the regime switch for each level  $j$ .

It is worth noticing that Eq. (5) becomes the following:  $\widehat{\text{CP}}_{ij} = \arg \min_{t \in \{1, \dots, T\}} \{\mathbf{1}(y_{ijt} < \hat{\gamma}_j)\}$  when the first regime in the time series is the upper regime.

## 5 Monte Carlo simulation study

We explore finite sample performance of the developed FD-IV-GMM estimator in Eq. (4). To this end, we perform a Monte Carlo study and investigate the performance of our proposal in terms of bias and mean squared error of the estimator for  $\beta, \delta_I, \delta_X, \gamma$ , and CP. The developed FD-IV-GMM estimator, the function to randomly generate data from the model in Eq. (1) as well as the performance measures used in this section have been implemented in the R package `PanelTM` submitted to CRAN.

We consider two different data generating processes (DGPs), one without time-varying regressors (DGP1) and the other with time-varying regressors (DGP2). We assume that the error term is distributed as a Gaussian white noise, that is  $\varepsilon_{ijt} \sim \mathcal{GWN}(0, 1), \forall j = 1, \dots, J$ . As for the DGP2, we assume the regressor  $X_{ijt}$  is distributed as a stationary autoregressive model,  $AR(1)$ , with coefficient equal to 0.7. We simulate different scenarios by varying sample size  $n$  in (50, 150) and time series length  $T$  in (11, 50), for each level  $j$ . We also vary the time-varying exogenous regressor coefficients and the threshold parameter across  $j$ 's values (see specific parameters values in the scenarios listed below). Moreover, when simulated time series are short, i.e.  $T = 11$ , the true value used for the change point is  $CP_{ij} = 8$ , while, when  $T = 50$ ,  $CP_{ij} = 20$ , for all  $i = 1, \dots, n$  and  $j = 1, \dots, J$ . In addition, we also carry out a Monte Carlo study using parameters values estimated on the real data set analysed in Sect. 6 and choosing  $J = 7$  where each  $j$  corresponds to a different frequency of the FM spectroscopy (see DGP1, scenario 2., in the list below and Tab. 2 to see the true parameters values used). We thus simulate the following scenarios for the two DGPs:

- DGP1:

1. Eq. (1) with  $J = 2$  and without time-varying regressors:

$$\begin{aligned} y_{i1t} &= -\mathbb{1}\{y_{i1(t-1)} \leq 0\} + \mathbb{1}\{y_{i1(t-1)} > 0\} + \varepsilon_{i1t} \\ y_{i2t} &= -0.7\mathbb{1}\{y_{i2(t-1)} \leq 0\} + 1.8\mathbb{1}\{y_{i2(t-1)} > 0\} + \varepsilon_{i2t} \end{aligned}$$

2. Eq. (1) with  $J = 7$  and each value of  $j$  corresponds to a specific frequency of the FM spectroscopy (see Sect. 2); here the simulated scenario is inspired by the data set analysed in Sect. 6; therefore, we set  $n = 150, T = 50, CP_{ij} = 8, \forall i, j$  and use the following subset of frequencies:  $20Hz, 500Hz, 2100Hz, 5000Hz, 8000Hz, 18000Hz, 29000Hz$ ; the true values for  $\gamma_j, \delta_{Ij}$  and  $CP_j$  (see Tab. 2, column "True value") are accordingly selected among those estimated through the developed model (see Sect. 6 for details);

- DGP2:

1. Eq. (1) with  $J = 2$ , a time-varying regressor, and  $\gamma_j = 0, \forall j = 1, 2$ :

$$\begin{aligned} y_{i1t} &= (-1 - 0.2x_{i1t})\mathbb{1}\{y_{i1(t-1)} \leq 0\} + (1 + 0.2x_{i1t})\mathbb{1}\{y_{i1(t-1)} > 0\} + \varepsilon_{i1t} \\ y_{i2t} &= (-0.7 - 0.5x_{i2t})\mathbb{1}\{y_{i1(t-1)} \leq 0\} + (1.8 + 0.8x_{i2t})\mathbb{1}\{y_{i2(t-1)} > 0\} + \varepsilon_{i2t} \end{aligned}$$

2. Eq. (1) with  $J = 2$  and a time-varying regressor, and  $\gamma_1 \neq \gamma_2 \neq 0$ :

$$\begin{aligned} y_{i1t} &= (0.5 + 0.8x_{i1t})\mathbb{1}\{y_{i1(t-1)} \leq 3\} + (5 - 0.7x_{i1t})\mathbb{1}\{y_{i1(t-1)} > 3\} + \varepsilon_{i1t} \\ y_{i2t} &= (5 + 1.2x_{i2t})\mathbb{1}\{y_{i1(t-1)} \leq 10\} + (11 + 0.3x_{i2t})\mathbb{1}\{y_{i2(t-1)} > 10\} + \varepsilon_{i2t} \end{aligned}$$

3. Model as in the previous case (DGP2, scenario 2.) but with  $CP_{i1} \neq CP_{i2}, CP_{i1} = 20$ , and  $CP_{i2} = 30 \forall i$ ; for obvious reasons here we only simulate the case with  $T = 50$ .
4. Model as in the DGP2, scenario 2. but with  $CP_{i1} \neq CP_{i2}, CP_{i1} = 7$ , and  $CP_{i2} = 8 \forall i$ ; for obvious reasons here we only simulate the case with  $T = 11$ .

To assess the performance of the proposed model and its estimation we perform  $B = 500$  replications for each considered scenario and compute the relative bias (RB) and the relative mean root squared error (RRMSE) for each model's parameter and for the change point. The sample version of RB and RRMSE are as follows:

$$\widehat{\text{RB}} = \frac{1}{B} \sum_{b=1}^B \left( \frac{\hat{\psi}_b - \psi}{\psi} \right), \quad \widehat{\text{RRMSE}} = \sqrt{\frac{1}{B} \sum_{b=1}^B \left( \frac{\hat{\psi}_b - \psi}{\psi} \right)^2}$$

where  $\psi$  is one of the parameters in the model, i.e.  $\beta_j$ ,  $\delta_j$ ,  $\gamma_j$ ,  $CP_j$ , and  $\hat{\psi}_b$  is the corresponding estimated value at the  $b$ -th Monte Carlo replication.

Monte Carlo estimations results are shown in Tables from 1 to 6. Note that in order to clearly show the results of the estimation accuracy of the intercept and all coefficients of the model, we have indicated with  $\delta_{Ij}$  the difference between the lower and upper regime's intercept at the  $j$ -th level of the third way and with  $\delta_{Xj}$  the difference between the lower and upper regime's slope parameter for the  $j$ -th level.

Table 1: Simulation results for DGP1, scenario 1.: model in Eq. (1) with  $J = 2$  and without time-varying regressors. Note that \* indicates that a not relative version of the measure is computed due to null denominator.

| $n$ | $T$ | $j$ | Parameter     | True value | $\widehat{RB}$ | $\widehat{RRMSE}$ |
|-----|-----|-----|---------------|------------|----------------|-------------------|
| 50  | 11  | 1   | $\delta_{I1}$ | 2.0        | 0.209          | 0.531             |
| 50  | 11  | 1   | $\gamma_1$    | 0          | -0.234*        | 0.419*            |
| 50  | 11  | 1   | $CP_1$        | 8          | -0.053         | 0.098             |
| 50  | 11  | 2   | $\delta_{I2}$ | 2.5        | 0.098          | 0.494             |
| 50  | 11  | 2   | $\gamma_2$    | 0          | -0.184*        | 0.364*            |
| 50  | 11  | 2   | $CP_2$        | 8          | -0.052         | 0.099             |
| 50  | 50  | 1   | $\delta_{I1}$ | 2.0        | -1.469         | 1.527             |
| 50  | 50  | 1   | $\gamma_1$    | 0          | 0.236*         | 1.099*            |
| 50  | 50  | 1   | $CP_1$        | 20         | 0.253          | 0.478             |
| 50  | 50  | 2   | $\delta_{I2}$ | 2.5        | -1.580         | 1.606             |
| 50  | 50  | 2   | $\gamma_2$    | 0          | 0.546*         | 1.320*            |
| 50  | 50  | 2   | $CP_2$        | 20         | 0.229          | 0.444             |
| 150 | 11  | 1   | $\delta_{I1}$ | 2.0        | 0.237          | 0.254             |
| 150 | 11  | 1   | $\gamma_1$    | 0          | -0.057*        | 0.094*            |
| 150 | 11  | 1   | $CP_1$        | 8          | -0.012         | 0.021             |
| 150 | 11  | 2   | $\delta_{I2}$ | 2.5        | 0.166          | 0.188             |
| 150 | 11  | 2   | $\gamma_2$    | 0          | -0.039*        | 0.062*            |
| 150 | 11  | 2   | $CP_2$        | 8          | -0.012         | 0.019             |
| 150 | 50  | 1   | $\delta_{I1}$ | 2.0        | -0.366         | 0.419             |
| 150 | 50  | 1   | $\gamma_1$    | 0          | -0.552*        | 0.738*            |
| 150 | 50  | 1   | $CP_1$        | 20         | -0.101         | 0.185             |
| 150 | 50  | 2   | $\delta_{I2}$ | 2.5        | -0.496         | 0.537             |
| 150 | 50  | 2   | $\gamma_2$    | 0          | -0.428*        | 0.699*            |
| 150 | 50  | 2   | $CP_2$        | 20         | -0.098         | 0.205             |

Regarding DGP1, scenario 1. (simulation results in Tab. 1), it appears that the proposed model is able to find the true CP irrespective of the sample size and the time series length even though a slight worsening is present when  $n = T = 50$ . As for the estimation accuracy of model coefficients, the  $\widehat{RB}$  and the  $\widehat{RRMSE}$  of all the estimates show satisfactory values that further improve as  $n$  increases and the length of time series decreases. Also for  $\delta_{Ij}$  and  $\gamma_j$  the worst case is when  $n = T = 50$ , probably due to a too long time series w.r.t. the sample size. However, when  $n = 150$  and  $T = 50$  and very different threshold values as well as lower and upper regime' parameters are used to generate panel data by varying the level  $j$  (DGP1, scenario 2.), the proposed model shows very satisfactory results both for the estimation accuracy and the change point detection (see Table 2). Also in the DGP2, scenario 2. (simulation results in Tab. 3) the identified CPs are very close to the true ones. As expected, all the model parameters show the best performance when the sample size is big ( $n = 150$ ) and the time series is not short ( $T = 50$ ). In addition, the positive effect of increasing the sample size and shorting time series appears to be a bit milder than that observed in simulations of the DGP1. Finally,  $\beta_j$  coefficients are the only ones showing an accuracy that would deserve further study. However, the overall performance of the proposed model is very satisfactory and the introduction of a time-varying regressor does not show a negative impact on it. Very similar remarks can be made for the investigated scenario 2. of the DGP2 whose results are shown in Tab. 4. Finally, in

Table 2: Simulation results for DGP1, scenario 2.: model in Eq. (1) with  $J = 7$  frequencies of the FM spectroscopy (for details see the text of the section), and without time-varying regressors.

| $j$ | Hz    | Parameter     | True value | $\widehat{RB}$ | $\widehat{RRMSE}$ |
|-----|-------|---------------|------------|----------------|-------------------|
| 1   | 20    | $\delta_{I1}$ | 12046.52   | 0.003          | 0.078             |
| 1   | 20    | $\gamma_1$    | 17586.24   | -0.341         | 0.341             |
| 1   | 20    | $CP_1$        | 8          | -0.001         | 0.017             |
| 2   | 500   | $\delta_{I2}$ | 8900.07    | -0.007         | 0.105             |
| 2   | 500   | $\gamma_2$    | 14284.21   | -0.310         | 0.310             |
| 2   | 500   | $CP_2$        | 8          | -0.002         | 0.030             |
| 3   | 2100  | $\delta_{I3}$ | 4825.16    | -0.020         | 0.124             |
| 3   | 2100  | $\gamma_3$    | 9457.06    | -0.254         | 0.254             |
| 3   | 2100  | $CP_3$        | 8          | -0.004         | 0.038             |
| 4   | 5000  | $\delta_{I4}$ | 3480.00    | -0.020         | 0.080             |
| 4   | 5000  | $\gamma_4$    | 8061.00    | -0.215         | 0.215             |
| 4   | 5000  | $CP_4$        | 8          | 0.000          | 0.000             |
| 5   | 8000  | $\delta_{I5}$ | 2460.11    | -0.070         | 0.106             |
| 5   | 8000  | $\gamma_5$    | 6953.72    | -0.176         | 0.176             |
| 5   | 8000  | $CP_5$        | 8          | -0.000         | 0.000             |
| 6   | 18000 | $\delta_{I6}$ | 1396.59    | -0.000         | 0.136             |
| 6   | 18000 | $\gamma_6$    | 4556.48    | -0.152         | 0.152             |
| 6   | 18000 | $CP_6$        | 8          | -0.004         | 0.019             |
| 7   | 29000 | $\delta_{I7}$ | 721.49     | -0.059         | 0.168             |
| 7   | 29000 | $\gamma_7$    | 3598.10    | -0.099         | 0.099             |
| 7   | 29000 | $CP_7$        | 8          | -0.007         | 0.029             |

Tables (5) and (6) we present the Monte Carlo results for the two most general cases where  $\gamma_1 \neq \gamma_2 \neq 0$  and  $CP_{i1} \neq CP_{i2}$  and the model includes a time-varying regressor. These results confirm the satisfactory performance of the proposed model in terms of both the estimation accuracy and the change point detection.

## 6 Empirical analysis

We here present the application of the three-way panel regression model developed in Sect. 3 on the fruit bioimpedance data described in Sect. 2. We propose two alternative applications of Eq. (1) to the bananas' bioimpedance measurements  $y_{ijt}$ : a simplified model with no time-varying regressor and a model with one time-varying regressor, which is the fruit weight, say  $x_{it}$ . In both cases, the first three lags of the considered variables - i.e.,  $y_{ijt}$  for the model without regressors and  $y_{ijt}$  and  $x_{it}$  for the model with a time-varying regressor - have been chosen as instrumental variables  $\{z_{ijt}\}_{t=t_0}^T$ . Therefore, observations at  $t = 1, 2, 3$  have been excluded from the thresholds' identification.

The FD-IV-GMM estimates of the threshold parameters and of the difference between the slope parameters are shown in Fig. 3. Coherently with the spectroscopy,  $\hat{\gamma}_j$  decreases as  $j$  increases. Overall, the two models led to similar estimated threshold values, as shown in Fig. 3, left. However, based on the Gaussian z-test, the estimated coefficients of the model including the banana's weight  $x_{it}$  are not significant. We have 107 p-values for FM ranging from 0.45 to 0.96 and 103 for IA ranging from 0.60 to 0.97, and higher p-values are associated with lower frequencies. This result is reflected in the corresponding estimated values of  $\hat{\delta}_{Ij}$ , which do not exhibit a clear pattern (Fig. 3, middle). In contrast, a more regular pattern can be observed for models without time-varying regressors. We thus conclude that the weight of the fruit is not a good explanatory variable for bioimpedance.

As far as the comparison of the two instruments is concerned, the estimates overall appear very similar (Fig. 3, left). However, some dissimilarities emerge between the estimated  $\hat{\gamma}_j$  of the two instruments. Indeed, the estimated threshold curves of the IA and the FM coincide for  $js$  up to approximately 4500 Hz, when the

Table 3: Simulation results for DGP2, scenario 1.: model in Eq. (1) with  $J = 2$ , a time-varying regressor, and  $\gamma_j = 0, \forall j = 1, 2$ . Note that \* indicates that a not relative version of the measure is computed due to null denominator.

| $n$ | $T$ | $j$ | Parameter       | True value | $\widehat{\text{RB}}$ | $\widehat{\text{RRMSE}}$ |
|-----|-----|-----|-----------------|------------|-----------------------|--------------------------|
| 50  | 11  | 1   | $\beta_1$       | -0.2       | 1.151                 | 3.275                    |
| 50  | 11  | 1   | $\delta_{I1}$   | 2          | -0.236                | 0.681                    |
| 50  | 11  | 1   | $\delta_{X1}$   | 0.4        | 0.637                 | 2.361                    |
| 50  | 11  | 1   | $\gamma_1$      | 0          | -0.697*               | 0.920*                   |
| 50  | 11  | 1   | CP <sub>1</sub> | 8          | -0.147                | 0.195                    |
| 50  | 11  | 2   | $\beta_2$       | -0.5       | 0.353                 | 1.198                    |
| 50  | 11  | 2   | $\delta_{I2}$   | 2.5        | -0.129                | 0.602                    |
| 50  | 11  | 2   | $\delta_{X2}$   | 1.3        | 0.027                 | 0.790                    |
| 50  | 11  | 2   | $\gamma_2$      | 0          | -0.382*               | 0.592*                   |
| 50  | 11  | 2   | CP <sub>2</sub> | 8          | -0.077                | 0.121                    |
| 50  | 50  | 1   | $\beta_1$       | -0.2       | -0.838                | 2.714                    |
| 50  | 50  | 1   | $\delta_{I1}$   | 2          | -1.939                | 1.980                    |
| 50  | 50  | 1   | $\delta_{X1}$   | 0.4        | -0.646                | 1.541                    |
| 50  | 50  | 1   | $\gamma_1$      | 0          | 0.588*                | 1.127*                   |
| 50  | 50  | 1   | CP <sub>1</sub> | 20         | 0.371                 | 0.507                    |
| 50  | 50  | 2   | $\beta_2$       | -0.5       | 1.317                 | 3.511                    |
| 50  | 50  | 2   | $\delta_{I2}$   | 2.5        | -1.990                | 2.197                    |
| 50  | 50  | 2   | $\delta_{X2}$   | 1.3        | 0.499                 | 1.383                    |
| 50  | 50  | 2   | $\gamma_2$      | 0          | -0.080*               | 1.238*                   |
| 50  | 50  | 2   | CP <sub>2</sub> | 20         | 0.025                 | 0.295                    |
| 150 | 11  | 1   | $\beta_1$       | -0.2       | -0.489                | 0.847                    |
| 150 | 11  | 1   | $\delta_{I1}$   | 2          | 0.349                 | 0.522                    |
| 150 | 11  | 1   | $\delta_{X1}$   | 0.4        | -0.369                | 0.776                    |
| 150 | 11  | 1   | $\gamma_1$      | 0          | -0.361*               | 0.525*                   |
| 150 | 11  | 1   | CP <sub>1</sub> | 8          | -0.078                | 0.115                    |
| 150 | 11  | 2   | $\beta_2$       | -0.5       | -0.165                | 0.308                    |
| 150 | 11  | 2   | $\delta_{I2}$   | 2.5        | 0.127                 | 0.210                    |
| 150 | 11  | 2   | $\delta_{X2}$   | 1.3        | -0.197                | 0.303                    |
| 150 | 11  | 2   | $\gamma_2$      | 0          | -0.154*               | 0.241*                   |
| 150 | 11  | 2   | CP <sub>2</sub> | 8          | -0.031                | 0.049                    |
| 150 | 50  | 1   | $\beta_1$       | -0.2       | -0.221                | 1.512                    |
| 150 | 50  | 1   | $\delta_{I1}$   | 2          | -0.828                | 0.930                    |
| 150 | 50  | 1   | $\delta_{X1}$   | 0.4        | -0.197                | 0.839                    |
| 150 | 50  | 1   | $\gamma_1$      | 0          | 0.007*                | 0.812*                   |
| 150 | 50  | 1   | CP <sub>1</sub> | 20         | 0.082                 | 0.31                     |
| 150 | 50  | 2   | $\beta_2$       | -0.5       | 1.061                 | 1.507                    |
| 150 | 50  | 2   | $\delta_{I2}$   | 2.5        | -0.653                | 0.727                    |
| 150 | 50  | 2   | $\delta_{X2}$   | 1.3        | 0.377                 | 0.565                    |
| 150 | 50  | 2   | $\gamma_2$      | 0          | -0.18*                | 0.461*                   |
| 150 | 50  | 2   | CP <sub>2</sub> | 20         | -0.022                | 0.112                    |

FM's curves abruptly increase. From that point on, the difference between the IA and the FM progressively reduces, but  $\hat{\gamma}_j$  always appears slightly lower for the IA. This evidence can be traced back to a technical issue that emerged during the experiment with the FM. Indeed, minor changes in the placement of the electrodes may have affected the data collection. Nevertheless, this technical issue does not compromise the reliability of the instrument and does not affect statistical analysis. Therefore, we decided to keep the whole data in order to better show the differences between the IA and the FM.

Table 4: Simulation results for DGP2, scenario 2.: model in Eq. (1) with  $J = 2$ , a time-varying regressor,  $\gamma_1 \neq \gamma_2 \neq 0$ , and  $CP_{i1} = 20$ , and  $CP_{i2} = 30$ ,  $\forall i$ .

| $n$ | $T$ | $j$ | Parameter     | True value | $\widehat{\text{RB}}$ | $\widehat{\text{RRMSE}}$ |
|-----|-----|-----|---------------|------------|-----------------------|--------------------------|
| 50  | 11  | 1   | $\beta_1$     | 0.8        | 0.492                 | 1.199                    |
| 50  | 11  | 1   | $\delta_{I1}$ | 4.5        | -0.480                | 0.616                    |
| 50  | 11  | 1   | $\delta_{X1}$ | -1.5       | 0.386                 | 0.945                    |
| 50  | 11  | 1   | $\gamma_1$    | 3          | -0.399                | 0.505                    |
| 50  | 11  | 1   | $\text{CP}_1$ | 8          | -0.095                | 0.137                    |
| 50  | 11  | 2   | $\beta_2$     | 1.2        | 0.157                 | 1.155                    |
| 50  | 11  | 2   | $\delta_{I2}$ | 6          | -0.452                | 0.611                    |
| 50  | 11  | 2   | $\delta_{X2}$ | -0.9       | 0.015                 | 2.243                    |
| 50  | 11  | 2   | $\gamma_2$    | 10         | -0.293                | 0.341                    |
| 50  | 11  | 2   | $\text{CP}_2$ | 8          | -0.124                | 0.172                    |
| 50  | 50  | 1   | $\beta_1$     | 0.8        | -0.685                | 1.338                    |
| 50  | 50  | 1   | $\delta_{I1}$ | 4.5        | -1.672                | 1.704                    |
| 50  | 50  | 1   | $\delta_{X1}$ | -1.5       | -0.476                | 0.835                    |
| 50  | 50  | 1   | $\gamma_1$    | 3          | 0.141                 | 0.690                    |
| 50  | 50  | 1   | $\text{CP}_1$ | 20         | 0.240                 | 0.426                    |
| 50  | 50  | 2   | $\beta_2$     | 1.2        | -0.532                | 0.692                    |
| 50  | 50  | 2   | $\delta_{I2}$ | 6          | -1.325                | 1.340                    |
| 50  | 50  | 2   | $\delta_{X2}$ | -0.9       | -0.687                | 0.948                    |
| 50  | 50  | 2   | $\gamma_2$    | 10         | 0.013                 | 0.207                    |
| 50  | 50  | 2   | $\text{CP}_2$ | 20         | 0.396                 | 0.517                    |
| 150 | 11  | 1   | $\beta_1$     | 0.8        | -0.116                | 0.248                    |
| 150 | 11  | 1   | $\delta_{I1}$ | 4.5        | -0.084                | 0.123                    |
| 150 | 11  | 1   | $\delta_{X1}$ | -1.5       | -0.048                | 0.295                    |
| 150 | 11  | 1   | $\gamma_1$    | 3          | -0.153                | 0.211                    |
| 150 | 11  | 1   | $\text{CP}_1$ | 8          | -0.026                | 0.042                    |
| 150 | 11  | 2   | $\beta_2$     | 1.2        | 0.081                 | 0.228                    |
| 150 | 11  | 2   | $\delta_{I2}$ | 6          | -0.059                | 0.089                    |
| 150 | 11  | 2   | $\delta_{X2}$ | -0.9       | 0.046                 | 0.633                    |
| 150 | 11  | 2   | $\gamma_2$    | 10         | -0.137                | 0.166                    |
| 150 | 11  | 2   | $\text{CP}_2$ | 8          | -0.029                | 0.044                    |
| 150 | 50  | 1   | $\beta_1$     | 0.8        | 0.084                 | 0.541                    |
| 150 | 50  | 1   | $\delta_{I1}$ | 4.5        | -0.747                | 0.777                    |
| 150 | 50  | 1   | $\delta_{X1}$ | -1.5       | 0.011                 | 0.301                    |
| 150 | 50  | 1   | $\gamma_1$    | 3          | -0.255                | 0.394                    |
| 150 | 50  | 1   | $\text{CP}_1$ | 20         | -0.044                | 0.121                    |
| 150 | 50  | 2   | $\beta_2$     | 1.2        | -0.275                | 0.416                    |
| 150 | 50  | 2   | $\delta_{I2}$ | 6          | -1.164                | 1.172                    |
| 150 | 50  | 2   | $\delta_{X2}$ | -0.9       | -0.392                | 0.610                    |
| 150 | 50  | 2   | $\gamma_2$    | 10         | -0.065                | 0.241                    |
| 150 | 50  | 2   | $\text{CP}_2$ | 20         | 0.267                 | 0.447                    |

As discussed in Section 2 and shown in Fig. 2, for a fixed frequency  $j$ , the bioimpedance shows approximately the same trend for all bananas while the time series tend to flatten out as frequencies increase. Nevertheless, the developed method always identifies the thresholds. In this respect, the presence of a threshold effect has been tested by means of the linearity test described in Appendix B using 500 bootstrap replications. For both the analyzers and both the models, estimated  $p$ -values are almost always greater than 0.97, and therefore the test supports the presence of a threshold effect irrespective of the frequency. When considering the model including  $x_{it}$ , a different result is obtained for four frequencies  $j$  - namely

Table 5: Simulation results for DGP2, scenario 3.: model in Eq. (1) with  $J = 2$ , a time-varying regressor,  $\gamma_1 \neq \gamma_2 \neq 0$ , and  $CP_{i1} = 7$  and  $CP_{i2} = 8, \forall i$ .

| $n$ | $T$ | $j$ | Parameter     | True value | $\widehat{\text{RB}}$ | $\widehat{\text{RRMSE}}$ |
|-----|-----|-----|---------------|------------|-----------------------|--------------------------|
| 50  | 50  | 1   | $\beta_1$     | 0.8        | -0.746                | 1.272                    |
| 50  | 50  | 1   | $\delta_{I1}$ | 4.5        | -1.688                | 1.712                    |
| 50  | 50  | 1   | $\delta_{X1}$ | -1.5       | -0.473                | 0.787                    |
| 50  | 50  | 1   | $\gamma_1$    | 3          | 0.194                 | 0.669                    |
| 50  | 50  | 1   | $\text{CP}_1$ | 20         | 0.269                 | 0.438                    |
| 50  | 50  | 2   | $\beta_2$     | 1.2        | -0.328                | 0.535                    |
| 50  | 50  | 2   | $\delta_{I2}$ | 6          | -1.409                | 1.424                    |
| 50  | 50  | 2   | $\delta_{X2}$ | -0.9       | -0.532                | 0.889                    |
| 50  | 50  | 2   | $\gamma_2$    | 10         | -0.151                | 0.282                    |
| 50  | 50  | 2   | $\text{CP}_2$ | 30         | 0.005                 | 0.196                    |
| 150 | 50  | 1   | $\beta_1$     | 0.8        | -0.211                | 0.314                    |
| 150 | 50  | 1   | $\delta_{I1}$ | 4.5        | -0.057                | 0.104                    |
| 150 | 50  | 1   | $\delta_{X1}$ | -1.5       | -0.179                | 0.287                    |
| 150 | 50  | 1   | $\gamma_1$    | 3          | -0.088                | 0.246                    |
| 150 | 50  | 1   | $\text{CP}_1$ | 20         | -0.656                | 0.656                    |
| 150 | 50  | 2   | $\beta_2$     | 1.2        | 0.104                 | 0.226                    |
| 150 | 50  | 2   | $\delta_{I2}$ | 6          | -0.064                | 0.093                    |
| 150 | 50  | 2   | $\delta_{X2}$ | -0.9       | 0.065                 | 0.565                    |
| 150 | 50  | 2   | $\gamma_2$    | 10         | -0.132                | 0.159                    |
| 150 | 50  | 2   | $\text{CP}_2$ | 30         | -0.740                | 0.740                    |

Table 6: Simulation results for DGP2, scenario 4.: model in Eq. (1) with  $J = 2$  and a time-varying regressor,  $\gamma_1 \neq \gamma_2 \neq 0$ ,  $CP_{i1} = 20$ ,  $CP_{i2} = 30, \forall i$ .

| $n$ | $T$ | $j$ | Parameter     | True value | $\widehat{\text{RB}}$ | $\widehat{\text{RRMSE}}$ |
|-----|-----|-----|---------------|------------|-----------------------|--------------------------|
| 50  | 11  | 1   | $\beta_1$     | 0.8        | 0.574                 | 1.483                    |
| 50  | 11  | 1   | $\delta_{I1}$ | 4.5        | -0.478                | 0.666                    |
| 50  | 11  | 1   | $\delta_{X1}$ | -1.5       | 0.327                 | 1.034                    |
| 50  | 11  | 1   | $\gamma_1$    | 3          | -0.267                | 0.571                    |
| 50  | 11  | 1   | $\text{CP}_1$ | 7          | -0.075                | 0.134                    |
| 50  | 11  | 2   | $\beta_2$     | 1.2        | 0.154                 | 1.115                    |
| 50  | 11  | 2   | $\delta_{I2}$ | 6          | -0.424                | 0.587                    |
| 50  | 11  | 2   | $\delta_{X2}$ | -0.9       | 0.027                 | 2.291                    |
| 50  | 11  | 2   | $\gamma_2$    | 10         | -0.278                | 0.328                    |
| 50  | 11  | 2   | $\text{CP}_2$ | 8          | -0.114                | 0.165                    |
| 150 | 11  | 1   | $\beta_1$     | 0.8        | -0.211                | 0.314                    |
| 150 | 11  | 1   | $\delta_{I1}$ | 4.5        | -0.057                | 0.104                    |
| 150 | 11  | 1   | $\delta_{X1}$ | -1.5       | -0.179                | 0.287                    |
| 150 | 11  | 1   | $\gamma_1$    | 3          | -0.088                | 0.246                    |
| 150 | 11  | 1   | $\text{CP}_1$ | 7          | -0.018                | 0.042                    |
| 150 | 11  | 2   | $\beta_2$     | 1.2        | 0.104                 | 0.226                    |
| 150 | 11  | 2   | $\delta_{I2}$ | 6          | -0.064                | 0.093                    |
| 150 | 11  | 2   | $\delta_{X2}$ | -0.9       | 0.065                 | 0.565                    |
| 150 | 11  | 2   | $\gamma_2$    | 10         | -0.132                | 0.159                    |
| 150 | 11  | 2   | $\text{CP}_2$ | 8          | -0.026                | 0.037                    |

4600, 4700, 4800, and 4900 Hz - of the FM. In such cases, the test does not reject the null hypothesis of linearity. However, it is worth noticing that this result is found in correspondence to frequencies  $j$  that were affected by the aforementioned technical issue in the FM experiment. Finally, we identify the time of regime

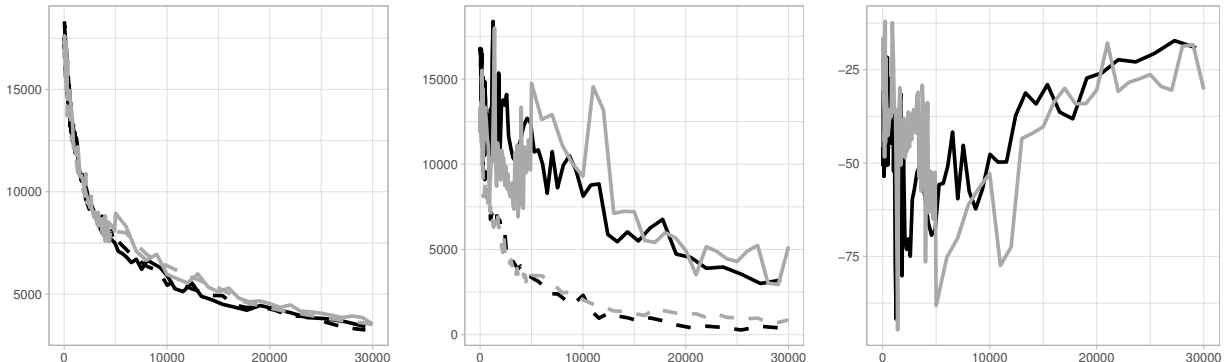


Figure 3: Logarithm of the considered estimated parameter (y-axis) per electrical frequency  $j$  (x-axis). Left: threshold parameters  $\hat{\gamma}_j$ . Middle: constants parameter  $\hat{\delta}_{Ij}$ . Right: weight's parameter  $\hat{\delta}_{Xj}$ . The black line refers to the IA and the grey line to the FM. The dashed lines report results from the model without time-varying regressors, and solid lines represent estimates from the model with a time-varying regressor.

switches according to the procedure described in Sect. 4. We first need to understand in what order the two regimes occur, whether upper first or lower first. Thus we compare the first observation -  $y_{ijt}$  at  $t = 4$  - with the corresponding estimated value  $\hat{\gamma}_j$ . If the observed value is lower (greater) than the estimated threshold parameter,  $t = 4$  belongs to the lower (upper) regime, and the change point is identified as the time  $t$  after which the longest sequence of days in the upper (lower) regime is observed. We then identify the change point for each banana  $i$  and frequency  $j$ , and then the average change point per each  $j$  as described in Sec. 4. The three-dimensional plots in Fig. 4 show the average time of regime switch for each  $j$  for the two considered models. It can be noticed a greater variability in the identified change points irrespective of the employed impedance analyzer when the model with a time-varying regressor is used. This finding is in line with the non-significance of the estimated coefficients of the fruit's weight. Overall, these results suggest that there is a physio-chemical change in the observed bananas approximately at day 7 for both the IA and the FM data.

## 7 Discussion and conclusion

In this paper, we have presented a three-way dynamic panel regression model with threshold effect. The third way is thought as a variable influencing the identification of the different regimes and their thresholds. Our proposal is thought also as a change point detection method. We have, indeed, defined a criterion to compute change points by varying the third way's level. To estimate the proposed model, the GMM estimation method in the instrumental variables framework has been implemented. Our model is, thus, able to take into account serial and cross-sectional dependence and provide information on the time when an abrupt change occurs by varying the level of a variable considered influential, in our case the frequency of the EIS. The model has been also empirically investigated through Monte Carlo simulations and the obtained results showed satisfactory performance in terms of both estimation accuracy and change point detected. From an applied viewpoint, the estimated model and the identified change point can be exploited to gain knowledge about the phenomenon under study. Moreover, the model and the change point detection criterion have been implemented in the R software package `PanelTM`.

Our proposal was directly motivated by an application to bioimpedance data analysis and showed good performances on three-way data concerning fruit bioimpedance experiment, both in terms of change times detected and interpretability of the results. From a statistical perspective, the bioimpedance data under investigation present some challenges as they are high-dimensional with a peculiar dependence structure

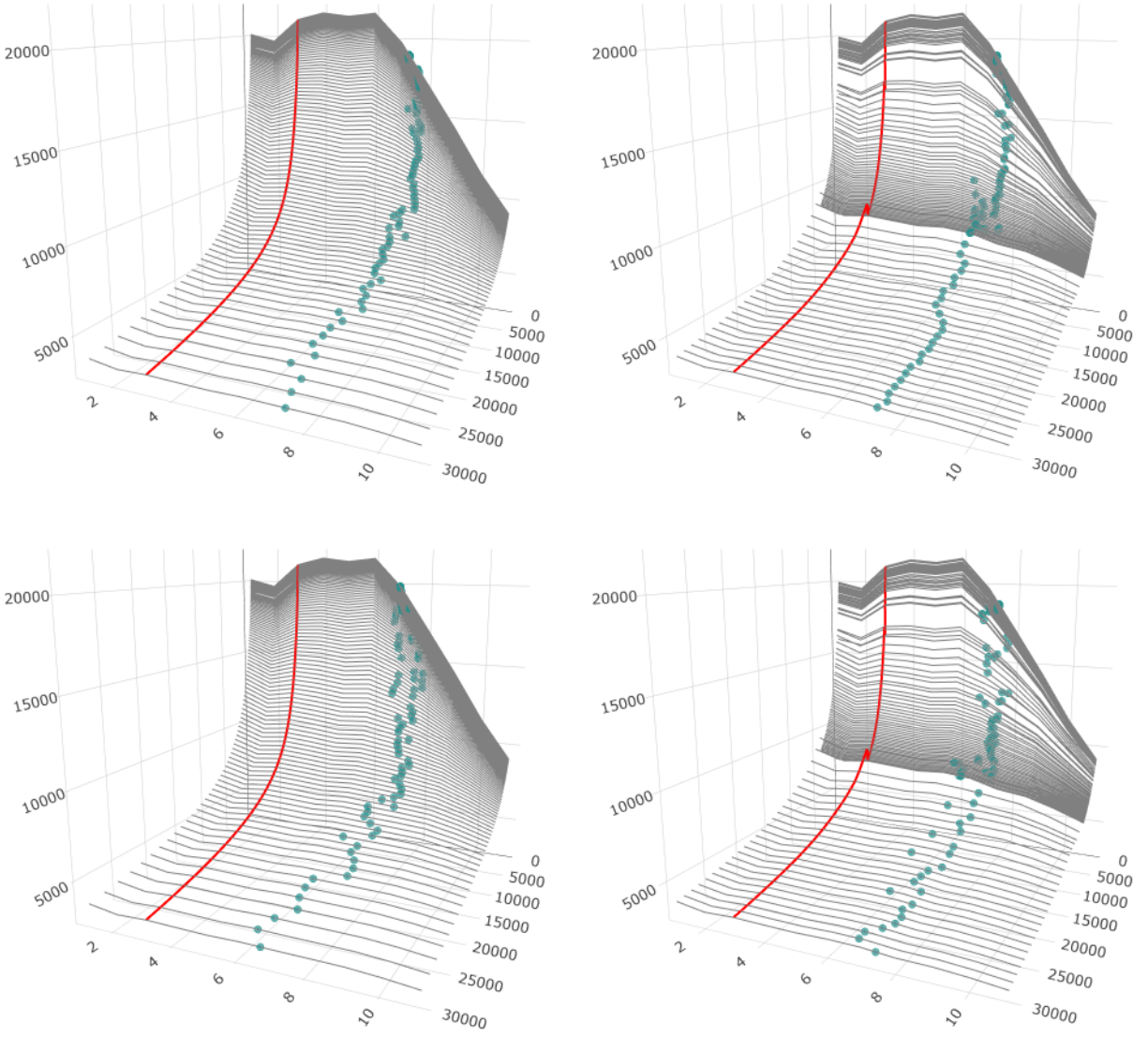


Figure 4: Average bananas bioimpedance (y-axis) per frequency  $j$  (z-axis) (grey lines) observed over time  $t = 1, \dots, 11$  (x-axis) and change points  $\widehat{CP}_j$  (green dots). The red line separates the observations used as instrumental variables from those used in the threshold estimation. Top: model without time-varying regressors. Bottom: model with a time-varying regressor. Left: IA. Right: FM.

over time and have possible change points. The model we introduced has been proven particularly useful in the given context since it has provided a meaningful characterization of the time series regimes. From a practical point of view, this allowed to gain relevant knowledge that in the future can be used to monitor the ripening process, help assess fruit ripeness, and determine the optimal harvest time, including preventing spoilage. Moreover, by comparing the results for two different impedance analyzers, it provided interesting insights about the performance of the portable EIS device, which is small, lightweight, easy to be transported and used in a wide range of situations and applications.

In principle, the proposed methodology can be useful to many other data sharing some characteristics with the bioimpedance data considered in this work. For example, in climate change studies, the temporal observation of debris flows, mudflows and snow avalanches, due to increasing frequency and intensity of heavy-to-extreme precipitation events, is crucial for assessing the hydrological response, e.g. land slope. In medical research, our threshold regression model may be used to study the response of patients before and after the administration of different levels of a drug for a given pathology. Other applications domains include, for example, economics, where the identification of a shock that increases/decreases industrial production while decreasing the unemployment rate or producer prices is crucial to an industry’s policy.

The proposed model can be thought of as a starting point when building new threshold regression models for multi-way data. Therefore, there are several possible future research directions for our work. An interesting extension consists in the exploration of models with multiple regimes, thresholds and, consequently, change points to be detected. This would require complicating the model by including a generic number of regimes and building change point detection tools aiming to identify multiple regime switches based on the temporal dynamics of the observed features. Another aspect worth examining is related to the assumption of independence between the levels of the third-way. Although this assumption allows model estimation to be implemented in parallel, thus reducing its computational burden, there are situations in which it is unrealistic. Relaxing this assumption is a great challenge that requires the minimization of the GMM objective function  $\hat{\mathbf{J}}(\boldsymbol{\theta})$ , which is not block diagonal as in Eq. (3) and should be minimized for all the  $J$  levels at the same time. In addition, the consistency and efficiency estimates of the  $J$  threshold parameters would also need to be proved. Finally, another possible research direction is concerned with the way the change point computation is thought of. The measures defined in Sect. 4 have been introduced as criteria to compute the change point on the basis of the estimated thresholds. The similar time series trends of the fruit bioimpedance analysed in the current work led to calculate a single change point for all the considered fruits. In other applied situations, this may not be correct because it would lose potentially valuable information about the cross-sectional variability of times at which a regime change occurs in the phenomenon under investigation. The matter here is to study a criterion more appropriate for cases where the time series in the panel show different trends.

## A Asymptotic theory

This section presents the asymptotic theory for the FD-IV-GMM estimator of the proposed model in Eq. (1).

It is well-known that the asymptotic theory of the GMM estimator based on the first-difference transformation has been already developed by Hansen (2000). In addition, the case of exogenous threshold variable has been largely investigated in the literature for static panel data models (Hansen, 1999), but there is also a huge literature on GMM estimation of linear dynamic panels (see, e.g., Arellano and Bond (1991); Blundell and Bond (1998); Hsiao and Zhang (2015)). Moreover, Seo and Shin (2016) developed the asymptotic theory for a dynamic panel threshold model, including consistent and efficient estimation of the threshold parameter, and provided the inference for threshold effects and endogeneity of the transition variable.

Focusing on the FD-IV-GMM estimator for a model where the threshold variable is endogenous, the theory in Seo and Shin (2016) is the starting point for the asymptotic theory of the proposed model. Since Eq. (1) assumes independence between the third-way levels, we estimate the model’s parameters for each third-way’s level  $j$  taken separately and, for each  $j$ , the standard GMM asymptotics as well as the FD-IV-GMM asymptotics are still valid. Thus the standard GMM asymptotics and the further development in Seo and Shin (2016) are also valid for the model in Eq. (1). Hence we can state that, for each  $j$ , ( $i$ ) the

FD-IV-GMM estimator always follows a normal distribution asymptotically:

$$\begin{pmatrix} \sqrt{n} \begin{pmatrix} \hat{\beta}_j - \beta_{jn} \\ \hat{\delta}_j - \delta_{j0} \end{pmatrix} \\ n^{1/2-\alpha}(\hat{\gamma}_j - \gamma_{j0}) \end{pmatrix} \xrightarrow[n \rightarrow \infty]{d} \mathcal{N}(0, (\mathbf{G}'_j \boldsymbol{\Omega}_j^{-1} \mathbf{G}_j)^{-1})$$

where the true value of  $\beta_j$  is fixed at  $\beta_{j0}$  while that of  $\delta_j$  depends on  $n$  such that  $\delta_{jn} = \delta_{j0}n^{-\alpha}$  for some  $0 \leq \alpha < 1/2$  and  $\delta_{j0} \neq 0$ ,  $\boldsymbol{\Omega}_j$  is finite and positive definite,  $\mathbf{G}_j = (\mathbf{G}_{\beta_j}, \mathbf{G}_{\delta_j}(\gamma_{j0}), \mathbf{G}_{\gamma_j}(\gamma_{j0}))$  is of full rank and it is composed by:

$$\mathbf{G}_{\beta_j} = \begin{bmatrix} -E(z_{ijt_0} \Delta \mathbf{x}'_{ijt_0}) \\ \vdots \\ -E(z_{ijT} \Delta \mathbf{x}'_{ijT}) \end{bmatrix}, \quad \mathbf{G}_{\delta_j}(\gamma_j) = \begin{bmatrix} -E(z_{ijt_0} \mathbf{1}_{ijt_0}(\gamma_j)' \mathbf{x}_{ijt_0}) \\ \vdots \\ -E(z_{ijT} \mathbf{1}_{ijT}(\gamma_j)' \mathbf{x}_{ijT}) \end{bmatrix},$$

and

$$\mathbf{G}_{\gamma_j}(\gamma_j) = \begin{bmatrix} \{E_{t_0-1}[z_{ijt_0}(\mathbf{1}_{ijt_0-1}, \mathbf{x}'_{ij(t_0-1)})|\gamma_j]p_{t_0-1}(\gamma_j) - E_{t_0}[z_{ijt_0}(\mathbf{1}_{ijt_0}, \mathbf{x}'_{ij(t_0)})|\gamma_j]p_{t_0}(\gamma_j)\} \delta_{0j} \\ \vdots \\ \{E_{T-1}[z_{ijT}(\mathbf{1}_{ijT-1}, \mathbf{x}'_{ij(T-1)})|\gamma_j]p_{T-1}(\gamma_j) - E_T[z_{ijT}(\mathbf{1}_{ijT}, \mathbf{x}'_{ijT})|\gamma_j]p_T(\gamma_j)\} \delta_{0j} \end{bmatrix},$$

where  $E_t[\cdot|\gamma_j]$  denotes the conditional expectation given  $y_{ij(t-1)} = \gamma_j$  and  $p_t(\cdot)$  the density of  $y_{ij(t-1)}$  assumed continuous and bounded, and  $\boldsymbol{\Omega}_j$  can be obtained as  $\mathbf{W}_n^{(j)-1}$ .

## B Testing for threshold effect

An important issue related to the three-way panel threshold model in Eq. (1) is to test whether there is a statistically significant change point in a sequence of chronologically ordered data. We here provide a testing procedure for the presence of the threshold effect based on a bootstrap algorithm and inspired by the work of Seo et al. (2019). For each  $j$ , we want to test the following hypothesis system:

$$\begin{cases} H_0 : \delta_{j0} = 0, \text{ for any } \gamma_j \in \Gamma_j \\ H_1 : \delta_{j0} \neq 0, \text{ for some } \gamma_j \in \Gamma_j \end{cases}$$

where  $\Gamma_j$  is the parametric space for  $\gamma_j$ . Using the standard approach based on the supremum statistics:

$$\sup \mathbf{W}_j = \sup_{\gamma_j \in \Gamma_j} \mathcal{W}_n(\gamma_j)$$

where  $\mathcal{W}_n(\gamma_j) = n \hat{\delta}_j(\gamma_j)' \hat{\boldsymbol{\Sigma}}_{\delta_j}(\gamma_j)^{-1} \hat{\delta}_j(\gamma_j)$  is the standard Wald statistic for each fixed  $\gamma_j$ ,

$$\hat{\boldsymbol{\Sigma}}_{\delta_j}(\gamma_j) = \mathbf{R} \left( \left( \hat{\boldsymbol{\Omega}}_j(\hat{\theta}_j(\gamma_j))^{-1/2} (\hat{\mathbf{G}}_{\beta_j}, \hat{\mathbf{G}}_{\delta_j}(\hat{\theta}_j(\gamma_j))) \right)' \left( \hat{\boldsymbol{\Omega}}_j(\hat{\theta}_j(\gamma_j))^{-1/2} (\hat{\mathbf{G}}_{\beta_j}, \hat{\mathbf{G}}_{\delta_j}(\hat{\theta}_j(\gamma_j))) \right) \right)^{-1} \mathbf{R}'$$

that is a consistent asymptotic variance estimator with  $\mathbf{R} = (\mathbf{0}_{(k_1+1)k_1}, \mathbf{I}_{k_1+1})$ .

To compute the statistic test, a bootstrap procedure is used. The main idea is that, the residuals  $\widehat{\Delta \varepsilon}_{ijt}$  from the original samples are used to compute  $\Delta y_{ijt}^* = \widehat{\Delta \varepsilon}_{ijt} \eta_i$  where  $\eta_i$ , with  $i = 1, \dots, n$ , are i.i.d. observations from the standard normal; next,  $\hat{\delta}_j(\gamma_j)^*$  and a bootstrap statistics  $\mathcal{W}_n^*(\gamma_j)$  are computed to get  $\sup \mathbf{W}_j^*$ . The empirical  $p$ -values of the test are computed as the proportion of suprema  $\sup \mathbf{W}_j^*$  (over  $\Gamma_j$ ) in the bootstrap replications that are bigger than  $\sup \mathbf{W}_j$ . This test has been implemented in the R software package `PanelTM`.

## Acknowledgments

This publication has emanated from research conducted with the financial support of the Free University of Bozen-Bolzano via the research project ‘‘New directions in statistical methods for bio-impedance analysis of fruit ripeness (BIOFRUIT - ID 2020)’’. The first author also acknowledges the financial support from the Italian Ministry of University and Research (MUR) under the Research Project of National Interest (PRIN) (grant 20223CEZSR) funded by European Union – Next Generation EU.

## References

- Arellano, M. and Bond, S. (1991). Some tests of specification for panel data: Monte carlo evidence and an application to employment equations. *Rev. Econom. Stud.*, 58:277–297.
- Bai, J. (2010). Common breaks in means and variances for panel data. *Journal of Econometrics*, 157:78–92.
- Balazsi, L., Matyas, L., and Wansbeek, T. (2018). The estimation of multidimensional fixed effects panel data models. *Econometric Reviews*, 37(3):212–227.
- Bardwell, L., Eckley, I., Fearnhead, P., Smith, S., and Spott, M. (2016). Most recent changepoint detection in panel data. *Technometrics*, 61.
- Blundell, R. and Bond, S. (1998). Initial conditions and moment restrictions in dynamic panel data models. *J. Econometrics*, 87:115–143.
- Casa, A., O’callaghan, T., and Murphy, T. (2022). Parsimonious bayesian factor analysis for modelling latent structures in spectroscopy data. *Annals of Applied Statistics*, 16(4):2417–2436.
- Chan, J., Horv ath, L., and Huřkov a, M. (2013). Darling–erdős limit results for change-point detection in panel data. *Journal of Statistical Planning and Inference*, 143:955–970.
- Chen, B. and Huang, L. (2017). Nonparametric testing for smooth structural changes in panel data models. *Journal of Econometrics*, 202.
- Cho, H. (2016). Change-point detection in panel data via double cusum statistic. *Electronic Journal of Statistics*, 10:2000–2038.
- El Khaled, D., Castellano, N., Gazquez, J., Garc a Salvador, R., and Manzano-Agugliaro, F. (2017). Cleaner quality control system using bioimpedance methods: a review for fruits and vegetables. *Journal of Cleaner Production*, 140:1749–1762.
- Grimnes, S. and Martinsen, O. (2015). *Bioimpedance and Bioelectricity Basics*, volume Biomedical Engineering. Academic, London, U.K.
- Grossi, M. and Ricc o, B. (2017). Electrical impedance spectroscopy (eis) for biological analysis and food characterization: A review. *J. Sensors Sensor Syst.*, 6(2):303–325.
- Hansen, B. (1999). Threshold effects in non-dynamic panels: Estimation, testing and inference. *J. Econometrics*, 93:345–368.
- Hansen, B. (2000). Sample splitting and threshold estimation. *Econometrica*, 68:757–603.
- Horv ath, L. and Huřkov a, M. (2012). Change-point detection in panel data. *Journal of Time Series Analysis*, 33(4):631–648.
- Hsiao, C. and Zhang, J. (2015). Iv,gmmor likelihood approach to estimate dynamic panel models when either n or t or both are large. *J. Econometrics*, 187:312–322.
- Ibba, P. (2021). *Fruit Quality Evaluation Using Electrical Impedance Spectroscopy*. PhD thesis, Free University of Bozen-Bolzano.
- Ibba, P., Crepaldi, M., Cantarella, G., Zini, G., Barcellona, A., Rivola, M., Petrelli, M., Petti, L., and Lugli, P. (2021). Design and validation of a portable ad5933-based impedance analyzer for smart agriculture. *IEEE Access*, 9:63656–63675.
- Ibba, P., Falco, A., Abera, B., Cantarella, G., Petti, L., and Lugli, P. (2020). Bio-impedance and circuit parameters: An analysis for tracking fruit ripening. *Postharvest Biology and Technology*, 159:110978.
- Li, D., Qian, J., and Su, L. (2015). Panel data models with interactive fixed effects and multiple structural breaks. *Journal of the American Statistical Association*.
- Maciak, M., Peřta, M., and Peřtov a, B. (2020). Changepoint in dependent and non-stationary panels. *Statistical Papers*, 61:1–23.
- M aty as, L. (1997). Proper econometric specification of the gravity model. *The World Economy*, 20:363–368.
- M aty as, L. (2017). *The Econometrics of Multi-dimensional Panels*, volume 50 of *Advanced Studies in Theoretical and Applied Econometrics*. Springer.
- Pliquett, U. (2010). Bioimpedance: A review for food processing. *Food Eng. Rev.*, 2(2):74–94.
- Seo, M., Kim, S., and Kim, Y.-J. (2019). Estimation of dynamic panel threshold model using stata. *The Stata Journal: Promoting communications on statistics and Stata*, 19:685–697.
- Seo, M. and Shin, Y. (2016). Dynamic panels with threshold effect and endogeneity. *Journal of Econometrics*, 195(2):169–186.
- Tom anek, P., Jan, M., Abubaker, H., and Grmela, L. (2010). Optical sensing of polarization states changes in meat due to the ageing. volume 1288, page 127 – 131.
- Tong, H. (1990). Non-linear time series: A dynamical system approach. *Oxford Statistical Science Series*, 6.